The Canadian Mineralogist
Vol. 36, pp. 701-711 (1998)

Mn–Fe SPINELS AND SILICATES IN MANGANESE-RICH ROCKS FROM THE OSSA–MORENA ZONE, SOUTHERN IBERIAN MASSIF, SOUTHWESTERN SPAIN

JUAN JIMÉNEZ-MILLÁN[1]

Departamento de Geología, Facultad de Ciencias Experimentales, Universidad de Jaén,
Campus Universitario, E-23071 Jaén, Spain

NICOLÁS VELILLA

Departamento de Mineralogía y Petrología, Facultad de Ciencias, Universidad de Granada, E-18002 Granada, Spain

ABSTRACT

Manganese-rich rocks occur in a greenschist-facies volcano-sedimentary complex of the Ossa–Morena Zone, in the Iberian Massif, southwestern Spain. Four unusually Fe-rich manganese associations containing Mn–Fe spinels and silicates have been identified: I) magnetite + pyroxmangite + spessartine + quartz, II) manganian jacobsite + pyroxmangite + aegirine + quartz, III) jacobsite + pyroxmangite + tephroite + spessartine + rhodochrosite, and IV) manganoan magnetite + rhodonite + ferroan tephroite + spessartine + rhodochrosite. Major compositional variations of these minerals are complex functions of several factors. Oxygen fugacity determines the Fe content of pyroxenoids in such a way that it is very low in the pyroxmangite of associations bearing Mn^{3+} spinels (<0.4 % $FeSiO_3$) and reaches 30% $FeSiO_3$ in associations with Fe^{2+}-dominant spinels. The presence of tephroite indicates $X(CO_2)$ values lower than 0.2, a condition that evolved toward higher values, as indicated by poikiloblasts of rhodonite. The most important effect of the whole-rock composition is the crystallization of tephroite in rocks with a Mn:Si ratio higher than 1.7. Local Ca availability determines the crystallization of rhodonite or pyroxmangite. In rocks with a low Mn:Fe ratio, the formation of tephroite is favored only when the accompanying pyroxenoid is rhodonite. In addition, in the absence of tephroite, the pyroxmangite is Fe-enriched (30% $FeSiO_3$), but in the absence of pyroxmangite, the tephroite may contain approximately 20% Fe_2SiO_4. The iron content of the garnet is controlled by coexisting minerals that preferentially partition Fe.

Keywords: Mn–Fe spinels, Mn–Fe silicates, Mn-rich rocks, chemical composition, $f(O_2)$, $X(CO_2)$, Iberian Massif, Spain.

SOMMAIRE

Des roches riches en manganèse ont été recristallisées dans le faciès schistes verts dans le complexe volcano-sédimentaire de la zone de Ossa–Morena, massif Iberique, dans le sud-ouest de l'Espagne. Nous décrivons quatre assemblages manganifères anormalement enrichis en fer contenant un spinelle et des silicates à Mn–Fe: I) magnétite + pyroxmangite + spessartine + quartz, II) jacobsite riche en Mn^{3+} + pyroxmangite + aegyrine + quartz, III) jacobsite + pyroxmangite + tephroïte + spessartine + rhodochrosite, et IV) magnétite manganifère + rhodonite + tephroïte ferreuse + spessartine + rhodochrosite. Les variations importantes dans la composition de ces minéraux semblent être des fonctions complexes de plusieurs variables. La fugacité de l'oxygène détermine la teneur en Fe des pyroxénoïdes de telle sorte qu'elle est très faible dans la pyroxmangite des associations contenant le spinelle riche en Mn^{3+} (<0.4 % $FeSiO_3$) et atteint 30% de $FeSiO_3$ dans les associations où le Fe^{2+} est dominant dans le spinelle. La présence de téphroïte indique des valeurs de $X(CO_2)$ inférieures à 0.2, condition qui a évolué vers des valeurs plus élevées, comme le témoigne le développement de poeciloblastes de rhodonite. L'influence la plus marquée de la composition globale des roches serait la cristallisation de la tephroïte dans les roches dont le rapport Mn:Si dépasse 1.7. La disponibilité locale du Ca détermine la cristallisation de la rhodonite ou de la pyroxmangite. Dans les roches à faible rapport Mn:Fe, la formation de la tephroïte est favorisée là où le pyroxénoïde qui l'accompagne est la rhodonite. De plus, en l'absence de tephroïte, la pyroxmangite est enrichie en fer (30% $FeSiO_3$), mais sans pyroxmangite, la tephroïte peut contenir environ 20% Fe_2SiO_4. La teneur en fer du grenat dépend de l'assemblage des minéraux coexistants qui pourraient capter le fer.

(Traduit par la Rédaction)

Mots-clés: spinelle à Mn–Fe, silicates à Mn–Fe, roches manganifères, composition chimique, $f(O_2)$, $X(CO_2)$, massif Ibérique, Espagne.

---

[1] *E-mail address*: jmillan@ujaen.es

INTRODUCTION

There are few reported associations of Fe and Mn spinels with Mn silicates and Mn carbonates. Most of the studies on such associations have been carried out in the Mn-rich rocks from the Sausar Group, India (Bhattacharya *et al.* 1988, Dasgupta *et al.* 1990, 1993) and Namibia (Bühn *et al.* 1995). The available data do not yet permit clarification of the influence of the controls of metamorphism [P, T, whole-rock composition, $f(O_2)$, $X(CO_2)$] and the crystal chemistry of the minerals have on the stability of the Mn and Fe phases, nor is the partitioning of elements among the phases well understood. There is a particular lack of knowledge concerning the effect of bulk chemical composition on the chemistry and stability of the minerals, as there have been few attempts to obtain individual chemical analyses of the microlayers characteristic of the associations of Mn and Fe minerals. In this sense, the papers of Huebner *et al.* (1992), Flohr & Huebner (1992) and Flohr (1992) have treated the chemical and mineral compositions of rocks in the system Mn–Si–O–Ca–(C). However, there are no references for studies of this type in relatively Fe-rich systems. This study is an attempt to improve knowledge of the relationships between the mineralogy and the chemical composition in Mn–Fe-rich systems. We examine four mineral associations in the central area of the Ossa–Morena zone, in southwestern Spain, characterized by the common presence of Mn–Fe spinels (jacobsite and magnetite) with Mn silicates (minerals of the pyroxenoid, olivine and garnet groups) and rhodochrosite.

GEOLOGICAL CONTEXT

The Ossa–Morena Zone is located in the southern part of the Iberian Massif. During the Hercynian Orogeny, this zone was partitioned into bands with fairly homogeneous internal tectonic–stratigraphic characteristics, although there are noticeable differences among them. The rocks studied occur in Oliva de la Frontera (province of Badajoz) and belong to the South–Central belt, one of the southernmost bands of the Ossa–Morena Zone (Fig. 1). These rocks occur in a tectonostratigraphic unit referred to as the Cumbres–Hinojales unit by Apalategui & Sánchez-Carretero (1991). This unit contains a Cambrian to early Devonian stratigraphic sequence metamorphosed to the greenschist facies. An Upper Cambrian – Lower Ordovician volcanosedimentary complex occurs within this unit and is characterized by silicic crystal metatuffs, slates and Mn- and Fe-rich lithologies: manganiferous metatuffs, Mn-bearing slates, coticules, braunite beds, hematite beds and rocks containing Mn-pyroxenoids and tephroite (Jiménez-Millán *et al.* 1992), which are the subjects of this study. These rocks occur in lenses less than 1 meter thick interbedded among metacherts and bands of coticules. Within these lenses, a centimeter-sized micro-scale banding is observed.

Two stages of Hercynian metamorphism have been identified (Vauchez 1975, Quesada & Munhá 1990). The first stage is evidenced by a foliation defined by the preferential orientation of the phyllosilicates in shaly lithologies. Manganese silicates crystallized along this foliation during the second stage of Hercynian metamorphism, which did not lead to foliation and was late- to post-tectonic in relation to the first deformation phase (Jiménez-Millán *et al.* 1994). The formation of the Mn minerals may be related to the existence of small thermal domes that, in this sector of the Ossa–Morena Zone, are considered responsible for assemblages postdating the main Hercynian phase of deformation (Quesada & Munhá 1990). The presence of spessartine in the rocks studied suggests a lower-temperature limit for this metamorphic event of approximately 400°C (Hsu 1968). However, since all of the samples studied are located very close together and since igneous bodies with contact metamorphic haloes are absent, the compositional differences among minerals cannot be explained by the effect of temperature gradients.

ANALYTICAL METHODS

The mineral compositions were determined using a Camebax SX–50 automated electron microprobe in the wavelength-dispersion mode operated under the following conditions: accelerating voltage 20 kV, probe current 5 nA, beam diameter 0.5 µm. The following compounds were used as calibration standards: albite, orthoclase, periclase, wollastonite and synthetic oxides (Al_2O_3, Fe_2O_3 and $MnTiO_3$).

Owing to the microbanded character of the rocks, bands with different mineral associations were separated before the chemical analysis of the rocks was carried out. The bands were cut into laminae and crushed, and a stereo microscope was used to hand-pick the purest portions of the complete associations for analysis. Whole-rock analyses were carried out at the X-Ray Assay Laboratories in Don Mills, Ontario using X-ray fluorescence for major elements.

PETROGRAPHY OF THE MANGANESE ASSOCIATIONS

In the study area, four mineral associations were distinguished in which minerals of the spinel and pyroxenoid groups coexist: I) magnetite + pyroxmangite + spessartine + quartz, II) manganian jacobsite + pyroxmangite + aegirine + quartz, III) jacobsite + pyroxmangite + tephroite + spessartine + rhodochrosite, and IV) manganoan magnetite + rhodonite + ferroan tephroite + spessartine + rhodochrosite.

The pyroxenoids pyroxmangite and rhodonite were optically distinguished according to the values of the

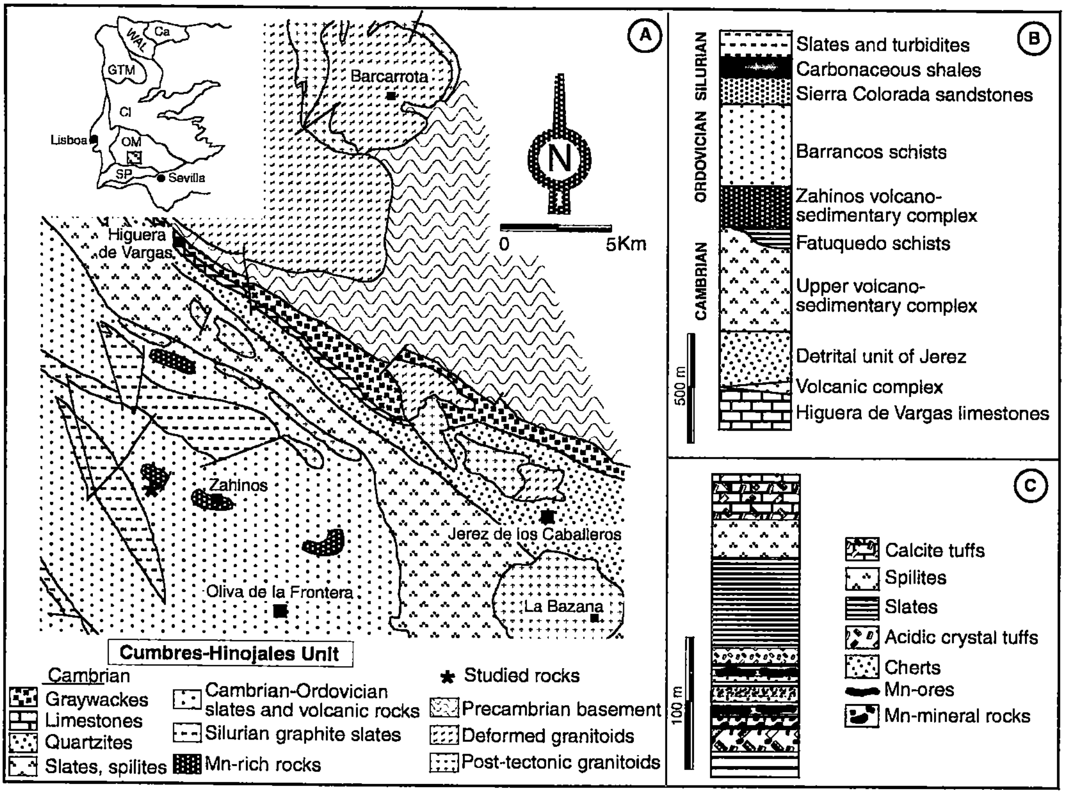

FIG. 1. A. Geological map of the Oliva de la Frontera area; SP: South Portuguese Zone; OM: Ossa–Morena Zone; CI: Central-Iberian Zone; GTM: Galicia Tras os Montes Zone; WAL: Western Astur-Leonese Zone; Ca: Cantabrian Zone. B. Stratigraphic column of the Cumbres–Hinojales Unit. C. Stratigraphic column of the Zahinos volcano-sedimentary complex. Based on Ruiz de Almodovar (1983) and Apalategui & Sánchez-Carretero (1991).

$2V$ angle, which is close to 90° in the case of the rhodonite and to 40° for the pyroxmangite. A significant fact is the presence of quartz in the two first associations, whereas in assemblages III and IV, an olivine-group mineral and rhodochrosite occur instead.

The rocks containing the type-I association develop a characteristic banding, centimeters thick, defined by layers very rich in spessartine (coticules) and discontinuous layers formed by a quartzitic matrix including the minerals of association I. The spessartine of the coticules has medium grain-size (<300 μm) and a mosaic texture. In the layers with a quartzitic matrix, there are also spessartine crystals, but they are euhedral, small (50 μm) and dispersed. The pyroxmangite appears as prismatic crystals up to 300 μm in size in contact with quartz or magnetite. The latter, in general, forms skeletal crystals ranging in size from 30 to 250 μm that may be replaced by hematite. Locally, there are some millimeter-sized lenticular aggregates very rich in magnetite.

The rocks containing the type-II association have a matrix mainly composed of small (70 μm) anhedral crystals of quartz and pyroxmangite. This matrix includes larger (200 μm) isolated crystals of manganian jacobsite, pyroxmangite and aegirine. The jacobsite appears as skeletal crystals, whereas pyroxmangite and aegirine are anhedral and contain abundant inclusions of quartz. In association II, a diffuse banding defined by variations in the modal concentration of jacobsite can be observed.

The type-III associations contain a matrix composed of small subhedral crystals of pyroxmangite and spessartine (< 80 μm). In this matrix, the rhodochrosite occupies an interstitial position of apparently residual character. Dispersed in the matrix are nodules several millimeters in size composed of anhedral crystals (150–200 μm) of tephroite and jacobsite, or of jacobsite alone. Exceptionally, in certain nodules, some jacobsite crystals are transformed to hematite parallel to various crystallographic planes.

Associations of type IV contain textures similar to those of type III. The matrix is also fine-grained (about 50 μm) and is composed of ferroan tephroite, magnetite, rhodochrosite and garnet. This matrix includes nodules several millimeters in size consisting of anhedral crystals of ferroan tephroite and magnetite up to 300 μm in size. The rhodochrosite is interstitial. The main textural difference between associations IV and III is the existence in IV of large anhedral poikiloblasts of rhodonite (600 μm) that include small crystals of the minerals that compose the matrix.

MINERAL CHEMISTRY AND WHOLE-ROCK COMPOSITION

The main mineral phases composing the above associations show major compositional variations, especially in the contents of Mn, Fe and Ca, as can be observed in representative results of electron-microprobe analyses of Mn silicates (Table 1) and oxides (Table 2).

In the pyroxenoids, the Ca content distinguishes the two structural types found. Thus, rhodonite (association IV) contains between 7% and 23% of the $CaSiO_3$ end-member (Fig. 2), whereas in pyroxmangite, the proportion of $CaSiO_3$ is always less than 3%. The high Ca content of the rhodonite contrasts with the contents that are usually described in pyroxenoids associated with rhodochrosite (see Mottana 1986, Flohr & Huebner 1992); it is more typical of pyroxenoids coexisting with Ca–Mn carbonates (Winter *et al.* 1981, Yui *et al.* 1989, Flohr 1992, Jiménez-Millán & Velilla 1993, 1994). On the other hand, the proportion of the $FeSiO_3$ end-member is a compositional parameter that clearly differentiates the pyroxmangite in various associations in the following order: Pxm II (<0.5% $FeSiO_3$) < Pxm III (5–9%) < Pxm I (22–30%). It is unusual that the highest Fe content observed here (association I) is more than twice as high as that of pyroxmangite associated with rhodochrosite and magnetite from Parseoni (Sausar Group, India: Dasgupta *et al.* 1993).

The olivine contains very low values of Mg/Mn, invariably less than 0.04. Its composition, therefore, corresponds to the fayalite–tephroite solid-solution series (Fig. 3) and, more specifically, to the Mn-rich side (Tep in the range 76–94). The ratio Mg/Mn is notably lower here than in olivine associated with oxides very rich in Mn (Ashley 1989, Lucchetti 1991, Jiménez-Millán & Velilla 1994), as well as in olivine associated with Fe-rich oxides (Dasgupta *et al.* 1993). Furthermore, the proportions of fayalite permit differentiation of two compositional fields: that of olivine in association IV, which varies between 18% and 24% Fa (ferroan tephroite), and that of the tephroite of association III, in which Fa is not higher than 7%.

Garnet occurs in three associations (I, III and IV) and, in all cases, it is very rich in Mn (between 2.50 and 2.85 *apfu*, atoms per formula unit) (Fig. 4). The Ca/(Ca + Mn) values vary from 0.08 to 0.27, hence the sum of the Mn end-members (spessartine + calderite) are invariably higher than 91%. These values correspond to the part richest in Mn of the compositional field of garnet associated with rhodochrosite (Dasgupta *et al.* 1987, Ashley 1989,

TABLE 1. REPRESENTATIVE COMPOSITIONS OF Mn-SILICATES, OSSA–MORENA ZONE, SPAIN

Mineral	Pyroxenoids				Garnets			Olivines	
Association	I	II	III	IV	I	III	IV	III	IV
SiO_2	46.36	46.86	46.17	46.78	35.93	35.44	35.86	29.91	29.81
TiO_2	-	-	-	-	0.52	0.42	0.28	-	-
Al_2O_3	-	-	-	-	17.57	16.12	17.53	-	-
FeO*	15.09	0.15	3.83	2.57	7.67	7.05	3.72	4.35	13.62
MnO	36.12	50.08	48.23	41.75	36.16	36.80	40.74	64.98	55.65
MgO	1.23	2.49	0.99	0.50	0.15	0.16	0.05	0.69	0.68
CaO	0.88	0.45	0.56	7.97	1.47	1.31	1.41	0.04	0.17
Total	99.68	100.03	99.78	99.57	99.47	97.30	99.59	99.97	99.93
Si	1.004	1.001	1.001	1.000	2.997	2.980	2.992	1.001	0.999
Ti	-	-	-	-	0.033	0.027	0.018	-	-
Al	-	-	-	-	1.728	1.597	1.722	-	-
Fe^{3+}**	-	-	-	-	0.272	0.403	0.260	-	-
Fe^{2+}**	0.273	0.003	0.064	0.046	0.263	0.093	-	0.122	0.382
Mn^{2+}	0.663	0.906	0.883	0.756	2.556	2.762	2.877	1.841	1.579
Mg	0.400	0.079	0.035	0.016	0.019	0.020	0.005	0.034	0.034
Ca	0.020	0.011	0.017	0.182	0.132	0.118	0.126	0.002	0.006

Results of electron-microprobe analyses are quoted in wt.% oxides. The structural formulae are based on 2 cations for the pyroxenoids, 8 cations for garnet and 3 cations for olivine-group minerals. * Total Fe as FeO. ** Inferred values based on charge-balance considerations.

TABLE 2. REPRESENTATIVE COMPOSITIONS OF OXIDES, OSSA–MORENA ZONE, SPAIN

Association	I		II		III		IV	
Analysis	1	2	3	4	5	6	7	8
SiO_2	0.16	0.27	0.13	0.05	0.03	0.05	0.04	0.02
TiO_2	0.50	0.23	0.57	0.58	0.40	0.65	0.55	0.39
Al_2O_3	0.10	0.12	0.26	0.24	0.16	0.08	0.07	0.04
Fe_2O_3	101.11	101.18	48.34	48.89	75.04	82.10	96.42	98.19
MnO	1.42	1.07	46.78	47.15	24.29	18.39	3.98	2.79
MgO	0.03	0.04	0.17	0.14	0.02	0.06	0.02	0.02
CaO	-	-	0.04	0.01	-	-	0.01	-
Total	103.32	102.91	96.29	97.06	99.94	101.33	101.09	101.45
Si	0.006	0.011	0.005	0.002	0.001	0.002	0.002	0.001
Ti	0.014	0.007	0.017	0.017	0.012	0.019	0.016	0.011
Al	0.005	0.005	0.012	0.011	0.007	0.003	0.003	0.002
Fe^{3+}**	1.954	1.960	1.414	1.420	1.967	1.956	1.961	1.974
Fe^{2+}**	0.973	0.980	-	-	0.216	0.419	0.884	0.918
Mn^{3+}**	-	-	0.530	0.531	-	-	-	-
Mn^{2+}**	0.046	0.035	1.010	1.010	0.796	0.599	0.132	0.093
Mg	0.002	0.002	0.010	0.008	0.001	0.003	0.001	0.001
Ca	-	-	0.002	-	-	0.000	0.001	-

Results of electron-microprobe analyses are quoted in wt.% oxides. Columns: 1 and 2: magnetite, 3 and 4: manganian jacobsite, 5 and 6: jacobsite, 7 and 8: manganoan magnetite. The structural formulae are based on 3 cations. * Total Fe is expressed as Fe_2O_3, and Mn, as MnO. ** Inferred values based on charge-balance considerations.

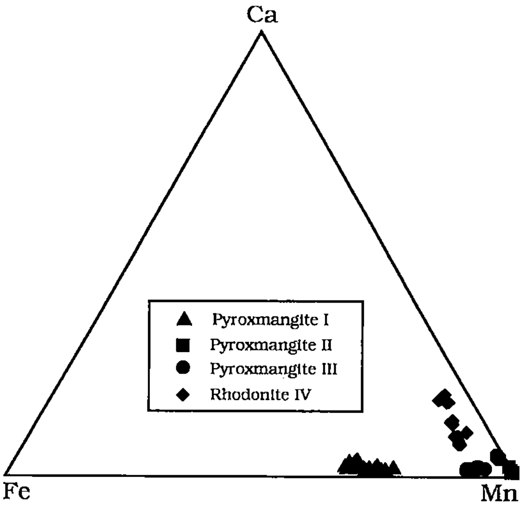

FIG. 2. Ca–Fe–Mn plot of pyroxenoid compositions from Ossa–Morena.

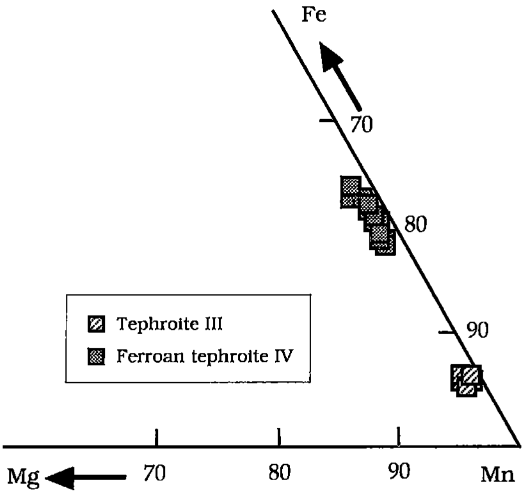

FIG. 3. Compositional variation of olivine minerals from Ossa–Morena.

Flohr 1992), although they are somewhat lower than in garnet of the coticules of Venn Stavelot (Belgium), which were considered by Schreyer *et al.* (1992) as formed from a rhodochrosite-rich precursor. The garnet of the associations with rhodochrosite (III and IV) can be differentiated according to their octahedral site occupancy. Thus, in the associations with magnetite (IV), the garnet has a higher Al content than that associated with jacobsite (III), which is more Fe-rich and contain over 0.31 *apfu* Fe^{3+}. This implies the

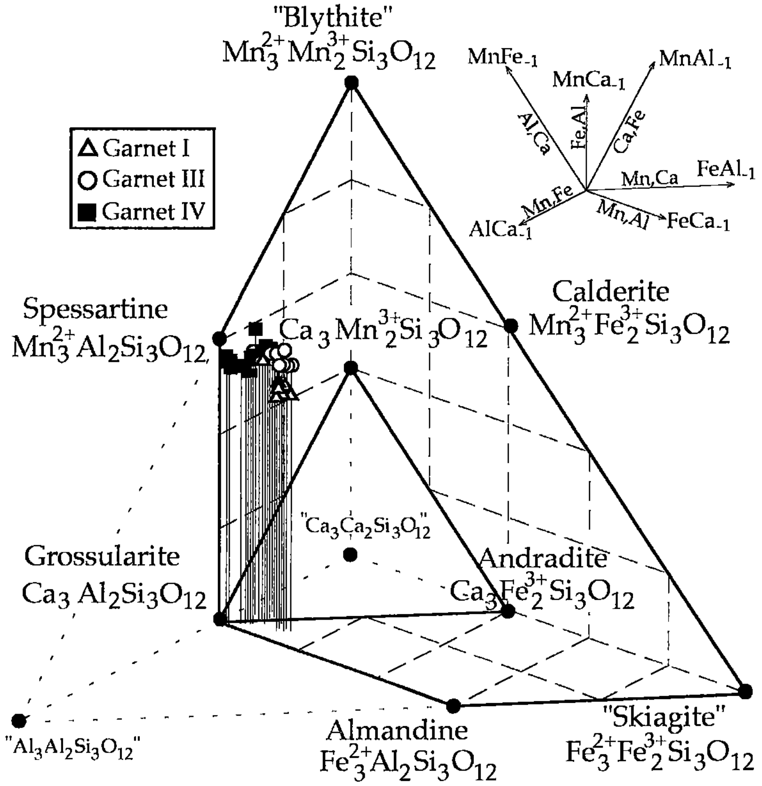

FIG. 4. Vector diagram showing compositional variation of garnet from Ossa–Morena.

presence of 4.5% to 18% of the calderite end-member in the garnet of the associations with jacobsite, as compared to 0–9% in the garnet associated with magnetite. In any case, these values are comparatively low compared to those of garnet in associations with rhodochrosite and jacobsite described by Dasgupta *et al.* (1987), where 52% of the calderite end-member is reached.

An unusual feature of the oxide compositions is the high proportion of the hausmannite end-member (28%) in spinel of association II, classified as manganian jacobsite, but spinel in the remaining associations does not contain Mn^{3+}. In the latter, the composition can be expressed within the series $Mn^{2+}Fe^{3+}_2O_4$ – $Fe^{2+}Fe^{3+}_2O_4$ (Fig. 5); the highest Mn content corresponds to jacobsite of association III. Within Mn^{3+}-free spinel, two compositional fields can be distinguished according to the proportion of the jacobsite end-member in solid solution. The Mn^{2+}-rich jacobsite contains between 77 and 79% $MnFe_2O_4$ (symbol IIIa in Fig. 5), and it is texturally characterized by the development of hematite lamellae along {111} and {100}, whereas in more Fe-rich jacobsite (53–59% $MnFe_2O_4$, symbol □ in Fig. 5) such lamellae are absent. The magnetite in association IV shows a moderate compositional interval (5–16% of jacobsite), whereas magnetite in association I is Mn-poor, and the proportion of jacobsite falls to below 2%.

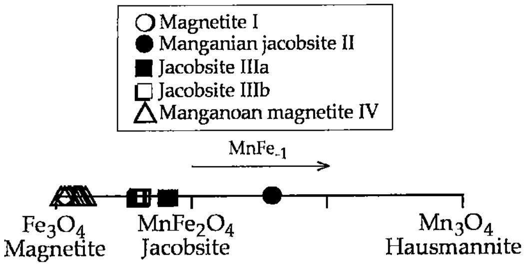

FIG. 5. Linear diagram showing the composition of the Fe–Mn spinel.

From a chemical point of view, the rocks are rich in Mn (34–48% MnO) and Fe (12–28% Fe_2O_3), and poor in Al (<8% Al_2O_3), Ca (<1.6% CaO), Mg and alkali elements (<1% of the respective oxides) (Table 3). These values fall within the interval typical of rocks with rhodochrosite and tephroite from other localities (Ashley 1989, Abrecht 1990, Flohr 1992). The high availability of Mn is evidenced by the high values of the ratios Mn/(Ca + Mn + Fe), higher than 0.6, and Mn/Si, higher than 0.7. Regarding the Fe content of the rocks, we can say that the Fe/(Ca + Mn + Fe) value is notably higher than that in other known manganese-rich rocks with similar associations of minerals (*e.g.*, Flohr 1992, Jiménez-Millán & Velilla 1994). The latter ratio shows a progressive variation according to the following order: IV (0.38) > II (0.31) > III,I (0.26–0.24). The low Ca content of the lithologies studied here is reflected in Ca/(Ca + Mn + Fe), which has a constant value of 0.02. These values are notably lower than those of other rocks containing tephroite, rhodonite and manganiferous spinel coexisting with calcite (Winter *et al.* 1981, Flohr 1992).

There are important differences in the distribution coefficients among minerals of the different associations, as well as between the whole-rock composition and that of the minerals. The lowest values of the $K_D^{\mathrm{Mn–Fe}}$ between the rock and each one of the various minerals [calculated as $(\mathrm{Mn/Fe})_{\mathrm{min}}/(\mathrm{Mn/Fe})_{\mathrm{rock}}$] always correspond to the spinels, in any association, with values lower than 0.5 (*i.e.*, spinel prefers Fe). If the partitions of these elements between pairs of silicates are considered, significant differences also are found, since the $K_D^{\mathrm{Mn–Fe}}$ between pyroxenoid and olivine has a value close to 1 in association III and is around 4 in association IV. In the garnet, the values of $K_D^{\mathrm{Mn–Fe}}$ between this mineral and olivine or pyroxenoid are invariably lower than 0.5 in all the associations (*i.e.*, garnet prefers Fe). Finally, $K_D^{\mathrm{Mn–Ca}}$ between pyroxenoid and garnet varies from 2.2 to 1.7 in associations I and III, but is not higher than 0.2 in association IV.

Effect of the Variables of Metamorphism on Stability and Composition of Minerals

Conditions of $f(O_2)$

The presence of certain phases and their chemical composition allow us to establish the conditions of oxygen fugacity, which played an important role in the stability of the Mn–Fe minerals. A first fact to consider is the absence of oxides very rich in Mn^{3+}, such as bixbyite or braunite, in equilibrium with the associations of the Oliva de la Frontera area, which fact indicates lower conditions of oxygen fugacity than those defined by the Mn_2O_3–Mn_3O_4 buffer. On the other hand, the compositional differences among the spinel-type oxides of the associations studied suggest important differences in the $f(O_2)$ conditions in which they were formed. Thus, the presence of Mn^{3+} and the absence of Fe^{2+} indicate relatively oxidizing conditions for the jacobsite of association II. Its high Mn^{3+} content, which is close to the maximum so far reported in the literature (Dasgupta *et al.* 1987), suggests that it formed at conditions close to the upper stability limit of jacobsite, estimated as being located about –17 log$f(O_2)$ at 400°C, two orders of magnitude above the Fe_2O_3–Fe_3O_4 buffer (Ono *et al.* 1971, Pelton *et al.* 1979).

TABLE 3. REPRESENTATIVE WHOLE-ROCK COMPOSITIONS (wt.%), OSSA–MORENA ZONE, SPAIN

Association	I	II	III	IV
SiO_2	33.20	14.20	36.08	25.50
Al_2O_3	8.36	2.58	4.85	4.04
CaO	1.13	1.59	1.33	1.09
MgO	0.36	0.61	1.23	0.70
Na_2O	0.09	1.00	0.12	0.12
K_2O	0.20	0.69	0.08	0.05
Fe_2O_3	12.58	24.25	14.97	27.26
MnO	34.60	47.29	37.09	38.59
TiO_2	0.50	0.22	0.17	0.23
P_2O_5	0.09	0.39	0.25	0.09

The composition of the spinel in the remaining associations (I, III and IV) indicates lower $f(O_2)$ conditions. In these cases, the Mn is always found as Mn^{2+}, which locates the upper stability limit of these associations below the Mn_3O_4–MnO buffer, corresponding to –29 log$f(O_2)$ at 400°C. Furthermore, the low content of the jacobsite end-member in magnetite of association I (<4.5%) and the high fayalite content in the olivine of association IV suggest that $f(O_2)$ conditions for both associations were clearly below the Fe_2O_3–Fe_3O_4 buffer. Such conditions were probably close to those of the QFM buffer, but the absence of quartz in association IV and the absence of an olivine-group mineral in association I do not allow confirmation of this inference.

It is clear that the oxygen fugacity exercises a strong control on the availability of Fe^{2+} in the system and, consequently, on the chemical composition of the pyroxenoids and the olivine-group mineral, since the structures of these minerals do not admit significant quantities of Fe^{3+}, although Mn ⇔ Fe^{2+} substitution is common (*e.g.*, Deer *et al.* 1978, 1982). This fact could explain the low Fe content of the Mn silicates formed in $f(O_2)$ high conditions (Ashley 1984, Jiménez-Millán & Velilla 1993, 1994). In the associations from Oliva de la Frontera, the effect of oxygen fugacity on the composition of Mn silicates is reflected by the compositional differences between the pyroxenoids of association II and those of associations I, III and IV. Thus, in association II, characterized by the presence of jacobsite rich in the hausmannite end-member (Fig. 4), pyroxmangite crystallized extremely impoverished in Fe^{2+} (<0.4% $FeSiO_3$ end-member) as compared to the composition of the pyroxenoids of the associations with Fe^{2+}-spinels (associations I and IV), crystallized at oxygen fugacity conditions below those of the hematite–magnetite buffer.

On the other hand, the lamellar intergrowths of hematite in some occurrences of jacobsite in association III mark a very local change in the $f(O_2)$ conditions that favored development of oxidation reactions and affected composition of this spinel. Thus, oxidation of the initial jacobsite gave way to the crystallization of hematite and more Mn-rich jacobsite, according to the following reaction proposed by Essene & Peacor (1983): $MnFe_2O_4 + O_2 = (Fe,Mn)_2O_3 + (Mn,Fe)_3O_4$.

Conditions of $X(CO_2)$

The experimental studies of the system Mn–Si–O–(C) (Muan 1959, Candia *et al.* 1975, Abs-Wurmbach *et al.* 1983) reveal that the association pyroxenoid + Mn spinel ± tephroite ± rhodochrosite can be formed a) by reduction reactions from a precursor rich in Mn-oxides, b) or by oxidation and decarbonation reactions from a carbonate-rich protolith.

The role of reduction processes has been illustrated by the petrographic studies of Ashley (1989) and Jiménez-Millán & Velilla (1994) on the crystallization of a tephroite-bearing paragenesis from a hausmannite-rich precursor, and also Jiménez-Millán & Velilla (1993), who described the appearance of rhodonite as a result of the reduction of braunite. On the other hand, the studies of Peters *et al.* (1973) and Bhattacharya *et al.* (1988) suggest the crystallization of pyroxenoid, olivine and spinel by successive prograde reactions involving decarbonation or oxidation (or both).

In the associations from the Oliva de la Frontera area, there is no textural evidence that tephroite was formed by reduction reactions involving Mn oxides, Mn silicates or quartz. The residual texture of the rhodochrosite in associations III and IV suggests that these parageneses are related to decarbonation processes of a precursor rich in carbonate and, probably, in Fe–Mn oxides.

In the case of decarbonation, the $X(CO_2)$ conditions exercise an important control on the stability and, therefore, on the order of crystallization of olivine and pyroxenoid. At fixed P and T, rhodochrosite and rhodonite react to form olivine when $X(CO_2)$ is lower than 0.2; at higher $X(CO_2)$ conditions, a pyroxenoid is the stable phase, whereas olivine is unstable (Candia *et al.* 1975). This finding suggests local differences of $X(CO_2)$ conditions among the studied associations. Thus, the olivine in associations III and IV indicates lower $X(CO_2)$ conditions (<0.2) than those of associations I and II, where olivine is absent. Both the textural arrangement of the ferroan tephroite, included in poikiloblasts of rhodonite, as well as the existence of a pyroxmangite-rich matrix that includes tephroite and jacobsite crystals, show that the $X(CO_2)$ conditions in association IV were unbuffered during metamorphism, and evolved toward higher $X(CO_2)$ values after the crystallization of the ferroan tephroite. This evolution is common in the metamorphism of rocks containing Mn silicates (Winter *et al.* 1981, Dasgupta *et al.* 1988, Jiménez-Millán & Velilla 1994). Nevertheless, other studies have documented stable $X(CO_2)$ conditions during metamorphism. Thus, Dasgupta *et al.* (1993) proposed that $X(CO_2)$ was buffered by mineral reactions to form Mn silicates in the rocks of Parseoni, India.

Effect of bulk composition

Bühn *et al.* (1995), among others, showed that compositional differences of Fe–Mn minerals in different types of rocks depend on the paragenesis, which is strongly controlled by initial differences in bulk composition and oxygen fugacity conditions among the protoliths. Thus, the crystallization of tephroite is restricted to very limited bulk compositions, for which the values of both Mn/Si and Mn/Fe are particularly important. The experimental studies of Muan (1959) and Abs-Wurmach *et al.* (1983), as well as its formula, show that progenitor materials with a Mn/Si ratio higher than 1 are required for the appearance of tephroite. This fact was also verified in various associations from the Hoskins mine, Australia (Ashley 1989), Sierra Nevada, California (Flohr 1992) and Aracena, Spain (Jiménez-Millán & Velilla 1994), in which the tephroite only formed in rocks with a Mn/Si value very much higher than 1. In agreement with these data, the tephroite-bearing associations from Oliva de la Frontera (III and IV) have bulk Mn/Si > 1.7, whereas those in which tephroite is absent (I and II) have bulk Mn/Si lower than 0.6. However, the Mn/Si values of associations I and II are higher than those of other rocks from this area characterized by the absence of pyroxenoids and the presence of spessartine or piemontite (or both) (Jiménez-Millán & Velilla 1993).

Dasgupta *et al.* (1993) have shown that the bulk Mn/Fe ratio also determines the stability of tephroite, since this phase admits Fe more easily than pyroxmangite and, therefore, is stabilized in Fe-rich bulk compositions. However, the data provided by the Oliva de la Frontera associations allow us to make additional observations.The range of Mn/Fe values in the tephroite-bearing associations (1.56–2.72) to a large extent overlaps the range encountered in tephroite-free associations (2.14–3.03). Furthermore, the $K_D^{\text{Mn–Fe}}$ values between pyroxenoid–olivine and mineral–rock show that Fe is not strongly partitioned by tephroite when the coexisting pyroxenoid is pyroxmangite ($K_{D\text{Px–Ol}}^{\text{Mn–Fe}} = 0.89$, $K_{D\text{Px–rock}}^{\text{Mn–Fe}} = 5.07$ and $K_{D\text{Ol–rock}}^{\text{Mn–Fe}} = 5.69$). However, this tendency changes when the pyroxenoid is rhodonite ($K_{D\text{Px–Ol}}^{\text{Mn–Fe}} = 3.98$, $K_{D\text{Px–rock}}^{\text{Mn–Fe}} = 10.53$ and $K_{D\text{Ol–rock}}^{\text{Mn–Fe}} = 2.65$). Therefore, we can conclude that in rocks with a low Mn/Fe value, the crystallization of tephroite is only favored when other physical and chemical conditions provoke the crystallization of rhodonite instead of pyroxmangite.

The crystallization of a specific type of pyroxenoid depends mainly on the availability of Ca in the metamorphic system. Abrecht & Peters (1975) and Abrecht (1988) concluded that at given pressure and temperature conditions, rhodonite is stabilized over pyroxmangite where significant quantities of Ca are available, whereas high contents of Fe and Mg increase the stability of pyroxmangite. In the manganese-rich rocks from the Aracena area (Jiménez-Millán & Velilla 1993, 1994), this hypothesis is confirmed by the crystallization of rhodonite in rocks with manganoan calcite and Ca/(Ca + Mn + Fe) higher than 0.7. However, this control over rhodonite–pyroxmangite crystallization is not directly reflected in association IV from the Oliva de la Frontera area, where the pyroxenoid is rhodonite despite the low Ca content of this association. Moreover, this Ca content is similar to those of associations I, II and III [Ca/(Ca + Mn + Fe) = 0.02] containing pyroxmangite. This apparent anomaly could be explained by taking into account the petrographic position of the pyroxenoid and the local availability of divalent elements at the moment of crystallization. Thus, the presence of large poikiloblasts of rhodonite indicates that its crystallization was subsequent to that of garnet and tephroite, which preferentially partitioned Mn, Fe and Mg, and provoked a late relative enrichment in Ca that favored the stabilization of rhodonite instead of pyroxmangite.

Influence of the mineral association

In previous paragraphs, we have described the influence of the bulk composition, $f(O_2)$ and $X(CO_2)$ on the stability and composition of the phases of the association. However, some of the compositional differences observed cannot directly be explained by the effect of these variables. This is the case of the differences in Fe contents of pyroxenoids from associations I, III and IV, and of olivine from associations III and IV. Thus, the Fe content of the pyroxenoid from association I (>22% $FeSiO_3$) is notably higher than those of the pyroxenoid from associations III and IV (<10% $FeSiO_3$). The high proportion of the fayalite component in tephroite from association IV (between 18 and 24%) in comparison with tephroite of association III (<6%) is also noteworthy. However, in all these associations the bulk Mn/(Mn + Fe) is very similar (about 0.7) and, furthermore, in all cases the $f(O_2)$ conditions guarantee a high availability for Fe^{2+} in the system. Therefore, neither of these parameters can be said to be responsible of the Fe enrichment. Data on the element distribution reveal that between coexisting pyroxmangite and tephroite, the partitioning of Fe is very similar ($K_{D\text{mineral-rock}}^{\text{Mn-Fe}}$) approximately 5). Therefore, the absence of one of these minerals permits a strong Fe enrichment in the other mineral that crystallizes. Thus, in association I, where tephroite is absent, probably due to high $X(CO_2)$ and a low bulk Mn/Si ratio, the $FeSiO_3$ component in pyroxmangite reaches 30%. However, in association IV, the $X(CO_2)$ conditions and the late availability of Ca determined that tephroite would be the first-crystallizing silicate and that the stable pyroxenoid would be rhodonite, which made possible the Fe enrichment in tephroite from this association.

In addition, the bulk-rock composition determines the crystallization and composition of other minerals that affect the composition of the garnet. In the rocks studied in this paper, the Fe^{3+} content of garnet from rhodochrosite-bearing rocks (associations III and IV) varies according to the mineral association that accompanies the garnet. Thus, the rocks with jacobsite (associations III), in spite of having a bulk Al/Fe ratio (about 0.25) higher than the rocks with manganoan magnetite (association IV) (about 0.10), contain garnet with a greater proportion of Fe^{3+}. This opposing trend between the garnet composition and the bulk composition of the system can be explained by taking into account the effect exercised by the bulk Mn/Fe value on the composition of the oxides and tephroite coexisting with the garnet. The high Mn/Fe value of the rocks with jacobsite (about 2.75) in comparison with the associations with magnetite (about 1.60) causes the crystallization of Fe-poor oxides and tephroite in the jacobsite-bearing associations, which permits a greater Fe entry into the coexisting garnet. Finally, the absence of silicates able to incorporate Fe^{3+} to a greater extent than garnet produces an enrichment in this ion in the garnet of association I. Ashley (1989) similarly noted the preference of Fe for garnet over coexisting minerals in the rocks of the Hoskin mine.

CONCLUSIONS

The most important factors in controlling the crystallization of tephroite in carbonate-rich protoliths were the low $X(CO_2)$ (<0.2) and the high Mn/Si ratio in the bulk composition (>1.7). The bulk Mn/Fe value favored the crystallization of tephroite instead of a pyroxenoid only where the pyroxenoid was rhodonite. Under given $f(O_2)$ conditions and bulk Mn/(Mn + Fe) value, olivine was enriched in Fe where rhodonite was stable.

A low bulk Mn/Si value allowed the crystallization of pyroxenoids. In the rocks studied here, this ratio generally had a value of around 0.5. Significant Ca was needed for rhodonite crystallization, either due to high original content, or because there was Ca enrichment at the time of crystallization. Oxygen fugacity was the most important determining factor of the Fe content of the pyroxenoids, because high $f(O_2)$ conditions prevented the existence of Fe^{2+} and, therefore, its incorporation into the pyroxenoids. Where the association was formed at lower $f(O_2)$ conditions, but with a similar bulk Mn/(Mn + Fe) value, the presence of tephroite produced Fe-depletion of the coexisting pyroxenoid, whereas its absence produced Fe-enrichment.

With regard to the garnet, the presence of phases that preferentially partitioned Fe (tephroite and oxides) caused Fe-impoverishment of the garnet, whereas the absence of silicates able to incorporate Fe^{3+} provoked an increase in the proportions of andradite and calderite components.

ACKNOWLEDGEMENTS

The authors are very grateful to Dr. D.M. Burt (Arizona State University) and an unnamed referee for careful reviewing the manuscript and their very useful suggestions. Financial support was provided by the Research Group RNM-179 of the *Junta de Andalucía* and the Project PB92–0961 D.G.I.C.Y.T.. We are grateful to Dr. Ian MacCandless of the University of Granada for his assistance in translating the original text.

REFERENCES

ABRECHT, J. (1988): Experimental evaluation of the $MnCO_3 + SiO_2 = MnSiO_3 + CO_2$ equilibrium at 1 kbar. *Am. Mineral.* **73**, 1285-1291.

________ (1990): An As-rich manganiferous mineral assemblage from the Ködnitz Valley (Eastern Alps, Austria): geology, mineralogy, genetic considerations, and implications for metamorphic Mn deposits. *Neues Jahrb. Mineral., Monatsh.*, 363-375.

________ & PETERS, T. (1975): Hydrothermal synthesis of pyroxenoids in the system $MnSiO_3$–$CaSiO_3$ at Pf = 2 Kb. *Contrib. Mineral. Petrol.* **50**, 241-246.

ABS-WURMBACH, I., PETERS, T., LANGER, K. & SCHREYER, W. (1983): Phase relations in the system Mn–Si–O: an experimental and petrological study. *Neues Jahrb. Mineral., Abh.* **146**, 258-279.

APALATEGUI, O. & SÁNCHEZ -CARRETERO, R. (1991): Síntesis y correlación de unidades en el borde meridional de la Zona de Ossa–Morena (ZOM): implicaciones geológicas. *Bol. Geol. Min. España* **102**, 339-347.

ASHLEY, P.M. (1984): Piemontite-bearing rocks from the Olary District, South Australia. *Aust. J. Earth Sci.* **31**, 203-216.

________ (1989): Geochemistry and mineralogy of tephroite-bearing rocks from the Hoskins manganese mine, New South Wales, Australia. *Neues Jahrb. Mineral., Abh.* **161**, 85-111.

BHATTACHARYA, P.K., DASGUPTA, S., CHATTOPADHYAY, G., BANERJEE, H., FUKUOKA, M. & ROY, S. (1988): Petrology of jacobsite bearing assemblages from Sausar Group, India. *Neues Jahrb. Mineral., Abh.* **159**, 101-111.

BÜHN, B., OKRUSCH, M., WOERMANN, E., LEHNERT, K. & HOERNES, S. (1995): Metamorphic evolution of neoproterozoic manganese formations and their country rocks at Otjosondu, Namibia. *J. Petrol.* **36**, 463-496.

CANDIA, M.A.F., PETERS, T. & VALARELLI, J.V. (1975): The experimental investigation of the reactions $MnCO_3 + SiO_2 = MnSiO_3 + CO_2$ and $MnSiO_3 + MnCO_3 = Mn_2SiO_4 + CO_2$ in CO_2/H_2O gas mixtures at a total pressure of 500 bars. *Contrib. Mineral. Petrol.* **52**, 261-266.

DASGUPTA, S., BANERJEE, H., BHATTACHARYA, P., FUKUOKA, M. & ROY, S. (1990): Petrogenesis of metamorphosed manganese deposits and the nature of precursor sediments. *Ore Geol. Rev.* **5**, 359-384.

________, BHATTACHARYA, P.K., CHATTOPADHAYAY, G., BANERJEE, H., MAJUMDAR, N., FUKUOKA, M. & ROY, S. (1988): Petrology of Mg–Mn amphibole-bearing assemblages in manganese silicate rocks of the Sausar Group, India. *Mineral. Mag.* **52**, 105-111.

________, ________, ________, FUKUOKA, M., BANERJEE, H. & ROY, S. (1987): Genetic reinterpretation of crystallographic intergrowths of jacobsite and hausmannite from natural assemblages. *Mineral. Petrol.* **37**, 109-116.

________, SENGUPTA, P., FUKUOKA, M. & ROY, S. (1993): Contrasting parageneses in the manganese silicate–carbonate rocks from Parseoni, Sausar Group, India and their interpretation. *Contrib. Mineral. Petrol.* **114**, 533-538.

DEER, W.A., HOWIE, R.A. & ZUSSMAN, J. (1978): *Rock-Forming Minerals.* **2A.** *Single-Chain Silicates.* Longman, London, U.K.

________, ________ & ________ (1982): *Rock-Forming Minerals.* **1A.** *Orthosilicates.* Longman, London, U.K.

ESSENE, E.J. & PEACOR, D.R. (1983): Crystal chemistry and petrology of co-existing galaxite and jacobsite and other spinel solution and solvi. *Am. Mineral.* **68**, 449-455.

FLOHR, M.J.K. (1992): Geochemistry and origin of the Bald Knob manganese deposit, North Carolina. *Econ. Geol.* **87**, 2023-2040.

________ & HUEBNER, J.S. (1992): Mineralogy and geochemistry of two metamorphosed sedimentary manganese deposits, Sierra Nevada, California, USA. *Lithos* **29**, 57-85.

HSU, L.C. (1968): Selected phase relationships in the system Al–Mn–Fe–Si–O–H: a model for garnet equilibria. *J. Petrol.* **9**, 40-83.

HUEBNER, J.S., FLOHR, M.J.K. & GROSSMAN, J.N. (1992): Chemical fluxes and origin of a manganese carbonate – oxide – silicate deposit in bedded chert. *Chem. Geol.* **100**, 93-118.

JIMÉNEZ-MILLÁN, J., JIMÉNEZ-ESPINOSA, R., VELILLA, N. & CHICA-OLMO, M. (1994): The use of correspondence analysis and principal component analysis as a tool for deducing metamorphic mineral crystallization in Mn-rich lithologies. *Terra Nova* **6**, 267-273.

________, RUIZ DE ALMODÓVAR, G. & VELILLA, N. (1992): Litologías manganesíferas del área central de Ossa–Morena (SW de Badajoz). *Geogaceta* **12**, 46-49.

________ & VELILLA, N. (1993): Compositional variation of piemontites from different Mn-rich rock-types of the Iberian Massif (SW Spain). *Eur. J. Mineral.* **5**, 961-970.

________ & ________ (1994): Mineralogy and geochemistry of reduced manganese carbonate – silicate-rocks from the Aracena area (Iberian Massif, SW Spain). *Neues Jahrb. Mineral., Abh.* **166**, 193-209.

LUCCHETTI, G. (1991): Tephroite from the Val Graveglia metacherts (Liguria, Italy): mineral data and reactions for Mn-silicates and Mn–Ca-carbonates. *Eur. J. Mineral.* **3**, 63-68.

MOTTANA, A. (1986): Blueschist-facies metamorphism of manganiferous cherts: a review of the alpine occurrences: *In* Blueschists and Eclogites (B.W. Evans & E.H. Brown, eds.). *Geol. Soc. Am., Mem.* **164**, 267-299.

MUAN, A. (1959): Phase equilibria in the system manganese oxide – SiO_2 in air. *Am. J. Sci.* **257**, 297-315.

ONO, K., UEDA, T., OZAKI, T., UEDA, Y., YAMAGUCHI, A. & MORIYAMA, J. (1971): Thermodynamic study of the iron – manganese – oxygen system. *J. Japan Inst. Metals* **35**, 757-763.

PELTON, A.D., SCHMALZRIED, H. & STICHER, J. (1979): Untersuchung der Thermodynamik der Spinelle Mn_3O_4–Co_3O_4, Fe_3O_4–Mn_3O_4 und Fe_3O_4–Co_3O_4 anhand einer Analyse der Phasendiagramme. *Berichte Bunsengesellschaft Phys. Chem.* **83**, 241-252.

PETERS, T., SCHWANDER, H. & TROMMSDORFF, V. (1973): Assemblages among tephroite, pyroxmangite, rhodochrosite, quartz: experimental data and occurrences in the Rhetic Alps. *Contrib. Mineral. Petrol.* **42**, 325-332.

QUESADA, C. & MUNHÁ, J. (1990): Ossa–Morena Zone. Metamorphism. *In* Pre-Mesozoic Geology of Iberia (R.D. Dallmeyer & E. Martínez García, eds.). Springer, Berlin, Germany (314-320).

RUIZ DE ALMODOVAR, G. (1983): *Mineralizaciones de Mn–Fe y de W en el área de Oliva de la Frontera, (SO. de Badajoz). Geología y génesis.* Ph.D. thesis, Univ. of Granada, Granada, Spain.

SCHREYER, W., BERNHARDT, H.-J. & MEDENBACH, O. (1992): Petrologic evidence for a rhodochrosite precursor of spessartine in coticules of the Venn–Stavelot Massif, Belgium. *Mineral. Mag.* **56**, 527-532.

VAUCHEZ, A. (1975): Tectoniques tangeantielles superposées dans le segment hercynien Sud-Iberique; les nappes et plis couchés de la region d'Alconchel – Fregenal de la Sierra (Badajoz). *Bol. Geol. Min. España* **86**, 13-20.

WINTER, G.A., ESSENE, E.J. & PEACOR, D.R. (1981): Carbonates and pyroxenoids from the manganese deposit near Bald Knob, North Carolina. *Am. Mineral.* **66**, 278-289.

YUI, TZEN-FU, LO, CHING-HUA & WANG LEE, CHIHMING (1989): Mineralogy and petrology of metamorphosed manganese-rich rocks in the area of Santzan River, eastern Taiwan. *Neues Jahrb. Mineral., Abh.* **160**, 249-268.

Received August 2, 1996, revised manuscript accepted March 31, 1998.